



Here, we employ a range of mass spectrometry (MS)-based analytical approaches to characterize the composition, stability, and processing of insect cell-derived hTRiC. We find that subunits are N-terminally processed, including methionine cleavage and acetylation, according to enzymatic regimes that are conserved in human cells. We identify and roughly quantify trace co-purifiers in the existing purification pipeline, including *T. ni* TRiC subunits and substrates. Lastly, we use native mass spectrometry to study the dissociation pathway of hTRiC. We show that following chemical disruption of the 16-mer, subunits can engage in re-formed canonical and non-canonical contacts; and we discuss potential implications for chaperonin assembly. These findings provide a resource and foundation for future exploration of TRiC assembly and function.

**C**  
by co-expressing CCT1-CCT8 as described

We purified human TRiC



the intact 16-mer (Fig. 2b; Supplementary Data 3). The human TRiC subunits were the eight most abundant proteins in both samples, comprising over 93% of the total protein in solution and over 95% in the excised gel sample. Small amounts of all eight insect cell TRiC subunits were also present, as were insect cell chaperones Hsp70 and Hsp90 (Supplementary Data 3). Tubulin, an obligate substrate of TRiC<sup>12</sup>, was also detected in both  $\alpha$ - and  $\beta$ -forms, comprising ~3% of the protein in solution and migrating with TRiC in the native gel (Fig. 2b; Supplementary Data 3). Whereas  $\alpha$ -tubulin levels in solution and in the complex were similar,  $\beta$ -tubulin was

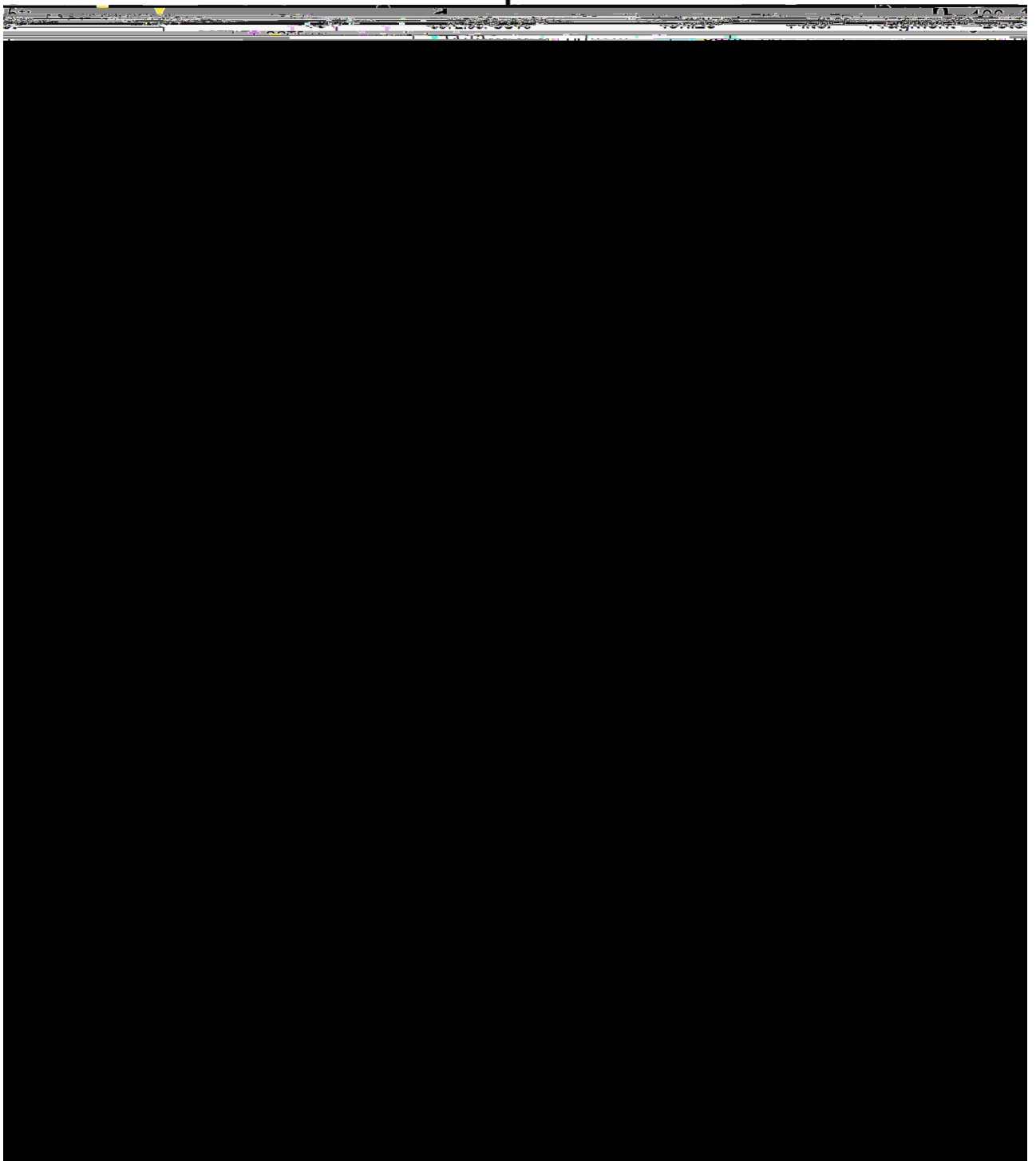


**Figure 3.** CCT5 is N-terminally processed by methionine excision and acetylation. **(a)** Schematic of the top-down MS experiment. The chaperonin is color-coded as though subunit identities are unknown. **(b)** Monomer region of the native mass spectrum of a hTRiC variant lacking subunits CCT2 and CCT4, containing predominantly CCT5 and trace amounts of other subunits (colored triangles). Each highlighted peak was fragmented. The inset is a magnified view of the most abundant charge state, 15<sup>+</sup>, showing that the resolution is high enough to distinguish sodium adducts. The CCT8 15<sup>+</sup> peak is just 3 m/z to the left of the peak of interest. **(c)** Deisotoped peptide spectrum resulting from fragmentation of the 15<sup>+</sup> peak in *b*. **(d)** Numbers of fragment ion matches from all highlighted peaks in *b* to sequences of all CCT subunits, divided into b- and y-ions. CCT2 and CCT4 are faded because they were not present in the sample, and can therefore serve as negative controls for the expected number of false positives. **(e)** Primary sequence of human CCT5 without the initiator methionine. Blue marks indicate at least one reported peptide mass (in data from all three highlighted peaks in *b*) supporting an N- or C-terminal ion cleaved at the given site. The red *N* at the N-terminus designates acetylation. **(f)** Measured and inferred N-terminal states of post-translationally processed recombinant hTRiC subunits expressed in insect cells. Red ovals denote acetylation.





amine was exposed, with the exception of the proportion of CCT3 beginning with glycine, a residue that is



functions<sup>51</sup>. Another early study also identified unassembled “micro-complexes” and, reasonably assuming that

of TRiC under a particular destabilizing condition as a sort of fingerprint could serve as a baseline for the re-addition of putative assembly factors in search of specific effects on intermediates that would be difficult to capture by alternative techniques.

Any intermediates in the course of forming an ordered hetero-oligomer are likely to be energetically favored only on the timescale of assembly to facilitate efficient formation of the final, functional products<sup>18,57</sup>. Thus, the apparent differences in stability that we observed—CCT5 and CCT8 among the most stable, CCT1 and CCT7 the least—may reflect these subunits' roles in the assembly process. Examining TRiC turnover and subcomplex formation using different combinations of CCT proteins and co-factors *in vivo* and *in vitro* will shed more light on its highly regulated assembly.





output was analyzed in Perseus v1.6.5<sup>65</sup>. Matches only identified by site; reverse matches; and contaminants were

25. Roh, S.-H. *et al.* Chaperonin TRiC/CCT modulates the folding and activity of leukemogenic fusion oncoprotein AML1-ETO. *J. Biol. Chem.* **291**, 4732–4741 (2016).
26. Serna, M. *et al.* The structure of the complex between alpha-tubulin, TBCE and TBCB reveals a tubulin dimer dissociation mechanism. *J. Cell Sci.* **128**, 1824–1834 (2015).
27. Stein, K. C., Kriel, A. & Frydman, J. Nascent polypeptide domain topology and elongation rate direct the cotranslational hierarchy of Hsp70 and TRiC/CCT. *Mol. Cell* **75**, 1117–1130 e5 (2019).
28. Melville, M. W., McClellan, A. J., Meyer, A. S., Darveau, A. & Frydman, J. The Hsp70 and TRiC/CCT chaperone systems cooperate in vivo to assemble the von Hippel-Lindau tumor suppressor complex. *Mol. Cell. Biol.* **23**, 3141–3151 (2003).
29. Cuellar, J. *et al.* The structure of CCT-Hsc70 NBD suggests a mechanism for Hsp70 delivery of substrates to the chaperonin. *Nat. Struct. Mol. Biol.* **15**, 858–864 (2008).
30. Frydman, J., Nimmegern, E., Ohtsuka, K. & Hartl, F. U. Folding of nascent polypeptide chains in a high molecular mass assembly with molecular chaperones. *Nature* **370**, 111–117 (1994).
- 31.

